4-1968

Kinetics of the Thermal Decomposition of Acetonitrile

Thomas William Asmus

KINETICS OF THE THERMAL DECOMPOSITION OF ACETONITRILE

by

Thomas William Asmus

A Thesis
Submitted to the
Faculty of the School of Graduate
Studies in partial fulfillment
of the
Degree of Master of Arts

Western Michigan University
Kalamazoo, Michigan
April 1968

ACKNOWLEDGEMENTS

The author wishes to express his appreciation to the members of his research committee, Dr. Donald Berndt and Dr. Robert Anderson and especially to Dr. Thomas Houser for his generous assistance and guidance. His wife, Mary Ann, is also gratefully acknowledged for the part that she played.

Thomas William Asmus

TABLE OF CONTENTS

LIST OF FIGURES

INTRODUCTION

This work involved the study of the kinetics of the thermal decomposition of acetonitrile in the gas phase using a stirred-flow reactor. Research was directed mainly at elucidating the mechanistic features of the reaction. Acetonitrile was selected for this project because its pyrolysis kinetics were unknown and because a relatively simple mechanism, leading to relatively few products, was anticipated.

Background

A thorough survey of the literature has failed to reveal any recent activity in the area of the kinetics of the thermal decomposition of acetonitrile although much work has been done on compounds of the same symmetry (C_3v) e.g., the methyl halides. Rabinovitch and Winkler[1], in 1942, studied this reaction at 865°C and atmospheric pressure with respect to the products of the thermal decomposition of acetonitrile but no mechanistic theory was forthcoming. These early investigators reported hydrogen, methane, and hydrogen cyanide as the major volatile reaction products. Acetylene and/or ethylene were reported as minor volatile products. The identities of these products were confirmed by standard combustion and absorption methods.

In 1958 E. E. McElcheran[2] et al. reported results of

the photolysis of acetonitrile at 1849 Å and suggested a mechanism to account for the products and observed kinetics. This technique led to the formation of some products which would not be expected to form under conditions necessary to affect thermal decomposition (except by the highly improbable third body collisions). These investigators suggested the following paths for initiation:

$$CH_3CN \begin{cases} \rightarrow H + CH_2CN \\ \rightarrow CH_3 + CN \end{cases}$$

where the former process was the most significant. The major product, hydrogen cyanide, was believed to be formed predominantly by a hydrogen atom abstraction of the CN group from acetonitrile.

The thermal decomposition of higher cyanides i.e., ethyl, t-butyl, and cumyl, have been investigated using the toluene carrier technique[3]; however, the results bore little relevance to this problem due to the preseuce of relatively weak carbon-carbon bonds in those molecules. The gamma ray decomposition of acetonitrile has been investigated[4], but no explicit mechanism has been proposed.

This compound, as an additive, has been found to improve fuel characteristics by lowering ignition temperatures and promoting smooth, non-explosive burning[5]. The explosive properties of mixtures of acetonitrile and nitric acid have been investigated also[6].

Kinetics in a Flow System

Flow systems are of two general types, those in which no stirring occurs in the reactor, i.e., plug-flow, and those in which sufficient stirring occurs so as to affect complete mixing within the reactor.

Considering a tubular reactor of constant cross-sectional area and flow conditions characterized by the former case, the change in the number of moles of component i with time in volume element (dV) is given by

$$dn_i/dt = r_i dV - udc_i \qquad (1)$$

where dV = cylindrical volume element

r_i = rate of chemical reaction

u = volume rate of flow of the reaction mixture

c_i = concentration of component i

At steady state, Eq. 1 becomes

$$r_i dV = udc_i$$

or

$$r_i = (u/dV)dc_i \qquad (2)$$

Under conditions of constant flow dV/u may be replaced by dt which gives the familiar closed-system kinetics equation, namely

$$r_i = dc_i/dt \qquad (3)$$

If one now considers a stirred-flow reactor in which the concentrations of reactant and products are considered uniform throughout and equal to the exit stream concentration, the volume element dV may be replaced by V (the total reactor volume), and dc_i may be replaced by $(c_i - c_o)$ giving

$$r = u(c_i - c_o)/V \tag{4}$$

where c_o = initial concentration of component i

Eq. 4 is applicable to any component of the system and if flow rates are assumed constant, it may be rewritten as

$$r = (c_i - c_o)/t \tag{5}$$

where t = contact time (average time a molecule resides in the reactor) = V/u

Eq. 5 enables explicit determination of reaction rate. Alteration of initial concentrations and/or flow rates permits determination of the form of the rate equation and rate constants without integration.

The above equations are applicable to reactions of any order and any degree of complexity. As an example, consider the following simple first order reaction:

$$A \longrightarrow B$$

for which $r = \text{rate} = -kc$ (6)

By combining Eqs. 3 and 6 and substituting dV/u for dt, the following differential equation applicable to tubular, plug-flow reactors is obtained:

$$-\frac{dc}{c} = \frac{k}{u}dV$$

This equation may be integrated over the reactor volume V_o; at the entrance to the reactor V = 0 and c = c_o (initial concentration of reactant), and at the exit $V = V_o$.

Therefore,

$$-\int_{c_o}^{c} \frac{dc}{c} = \frac{k}{u}\int_{0}^{V} dV$$

In this case integration gives

$$k = -(u/V)\ln(c/c_o) = -\frac{1}{t}\ln(c/c_o)$$

where c = concentration of A at contact time, t

For a stirred-flow reactor, Eqs. 5 and 6 are combined to give:

$$r = (c - c_o)/t = -kc$$

or

$$k = (c_o - c)/ct$$

Thus, the stirred-flow reactor offers the advantage of enabling direct determination of reaction rates from which rate constants and the order of the rate equation can be obtained without integration.

EXPERIMENTAL

Apparatus

A schematic representation of the flow system used for experimentation in this study is shown in Figure 1. The entire system was constructed of Pyrex tubing with the exception of the reactor which was made of Vycor, permitting reactor temperatures as high as 1200°C. In addition, Vycor is suitable for constant volume containers due to its very low coefficient of thermal expansion. The reactor and all cold traps were joined to the flow system by ball joint unions to facilitate quick changes and cleaning.

Helium was the sole carrier gas used and was purified in the flow system by transversing about 1 lineal foot of activated charcoal at liquid nitrogen temperatures. Carrier gas flow control was accomplished with a pressure regulator-needle valve combination. The helium flow was monitored with a calibrated capillary flow meter, F, containing di-n-butyl phthlate as the manometric fluid.

Prior to the injection of acetonitrile, the carrier gas was heated in an 8-inch-long preheater section to facilitate vaporization of the reacting species. The preheater consisted of 10 mm Pyrex tubing wrapped with 22 B & S gauge chromel resistance wire insulated by asbestos.

Acetonitrile was injected into the carrier gas stream at point S with a Sage model 237-2 motor driven, variable

LEGEND

C - Capillary
CF - Cold Finger
F - Flowmeter
P - Preheater
R - Reactor
S - Syringe
SC-3 - 3-way Stopcock
T_1, T_2, T_3, - Cold Traps
T(in) - Helium Purifier Trap
Th - Thermometer

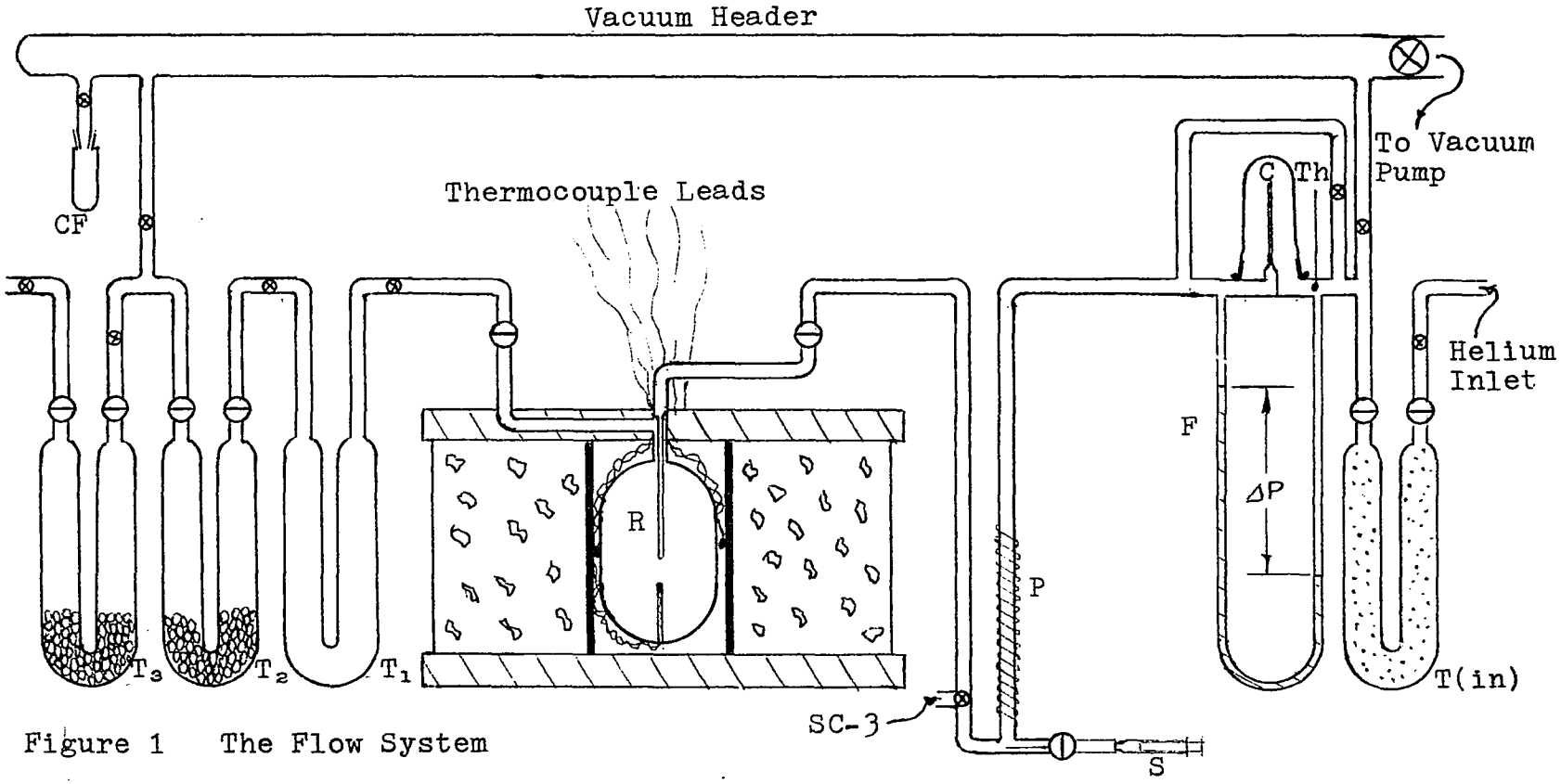

Figure 1 The Flow System

speed syringe drive. A 1.0 ml tuberculin syringe was connected to a hypodermic needle silver soldered into a metal ball joint which joined the needle and syringe assembly to the glass flow system. The rate of injection was determined by the syringe diameter, the gear configuration of the syringe drive, and the potentiometer setting which governed the speed of the drive motor. Injection was manually started and stopped over measured time intervals.

The gaseous mixture, having traveled about 2½ feet from the point of injection and around five 90° bends was assumed homogeneous at the reactor entrance. The bulb portion of the reactor, R, was 8 cm high and 4 cm in diameter and had an effective volume of 73 ± 2 ml. The uncertainty in the reactor volume arose from the temperature gradient established along the inlet and outlet paths. To facilitate stirring, the gaseous mixture entered the reactor through a centered 4 mm tube from which it jetted from pin holes near the reactor's center. Another 4 mm tube extended from the bottom to near the center of the reactor and served as a thermocouple well for temperature measurement. The reactor outlet was concentric with the inlet tube. In order that explicit determination of differential rate data be attainable from this system, it was imperative that the reactor design affect complete mixing of the contained gases i.e., that the concentrations of gaseous species in the exit stream were equal to those in the reactor. Experiments conducted by Sullivan and Houser[7] showed that the above assump-

tion was a valid one for the type of reactor described.

The reactor, shown schematically in Figure 2, was heated in an electric furnace formed by wrapping a 2 inch diameter (I.D.), ⅛ inch thick ceramic sleeve (Norton-Mullite) with two concentric windings (about 10 ohms each of 18 B & S gauge resistance wire) extending its full length. Sheet asbestos served as insulating material near the windings. The outer winding was powered by a heavy duty (2 KVA) variac which was connected directly to a 115 volt 60 cps line. The inner (controller) winding was powered by a variac (1 KVA) which was actuated (ON-OFF) by Honeywell Versatronik, model R7161H, temperature controller. A chromel-alumel thermocouple placed between the reactor and the furnace wall, was used as a temperature sensor for the controller. Three additional standardized (NBS - Zn, Pb, Cu, Al) chromel-alumel thermocouples were used for temperature measurement, two of which were placed in the thermocouple well of the reactor and the third inserted between the reactor and the furnace wall. The insulating portion of the furnace consisted of an 8 inch diameter by 6 inch high stainless steel housing with 1 inch thick transite discs covering each end. The heating element was concentric with the insulator housing and the resulting annular space was filled with Norton alundum abrasive grain 38X.

The trapping section consisted of three "U" traps, T_1, T_2, and T_3; T_2 and T_3 were filled with ⅛ inch glass

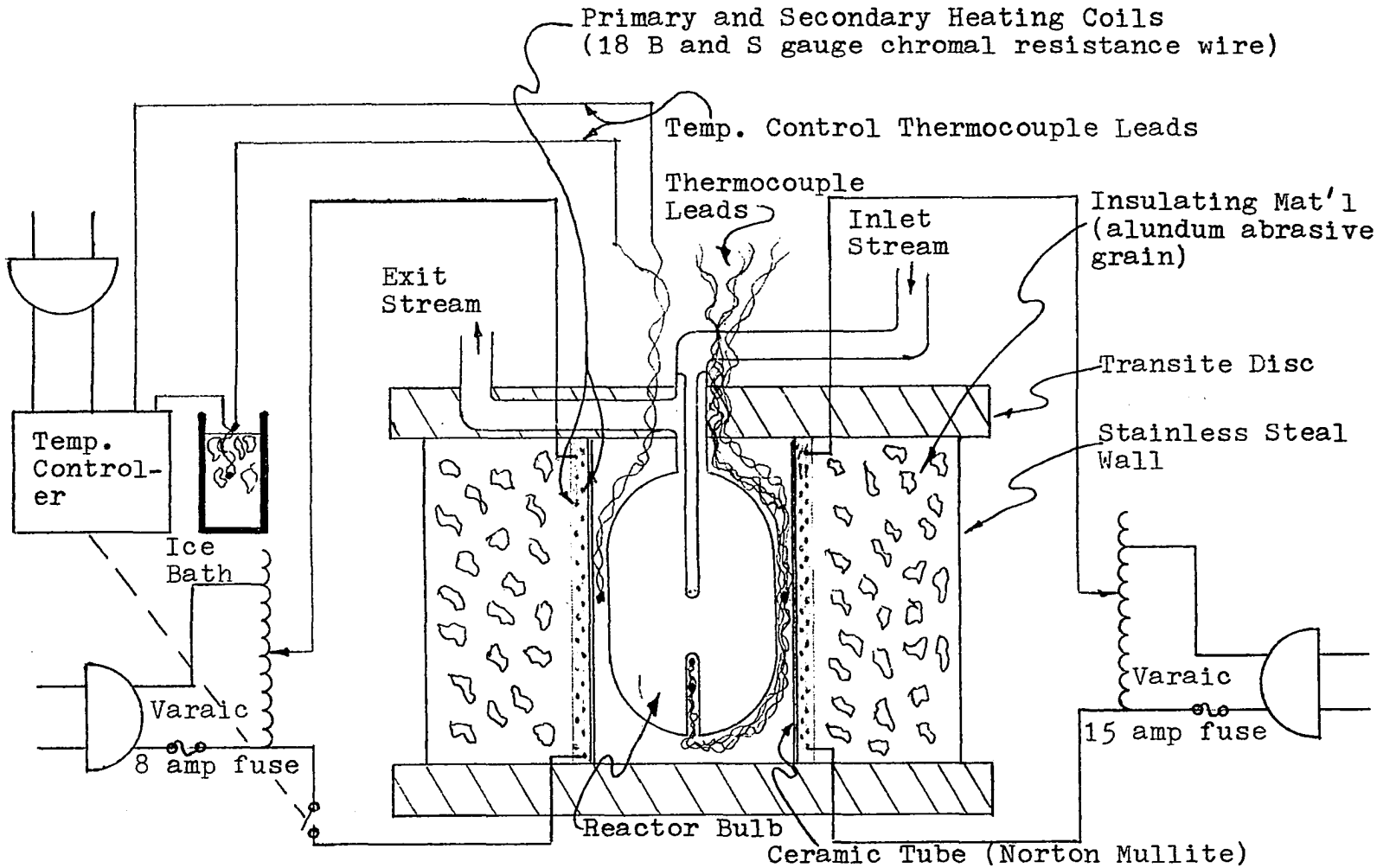

Figure 2 Reactor and Furnace Assembly

beads to increase the cold surface area. Liquid nitrogen was the coolant for these three traps.

The vacuum system, connected to the trapping section, provided for transfer, at room temperature, of the volatile reaction products plus unreacted acetonitrile to a cold finger, CF, (an evacuated small vial) cooled to liquid nitrogen temperatures. The vacuum system was evacuated by a Welch Duo Seal model 1405 vacuum pump.

Procedure

Run No. 1, which was typical of all subsequent runs with respect to technique, is cited as an example for the experimental procedure used. Attainment of the desired reactor temperature (in this case 880°C) was ascertained by measuring the thermocouple (inserted into the reactor's thermocouple well) output potential with a Honeywell model 2732 portable potentiometer. This corresponded to the number of degrees C above room temperature since the thermocouple's series cold junction was at room temperature. Thus, a thermocouple output (corresponding to 880 - 24 = 856°C) or 35.58 mv[8] was necessary, and the temperature controller was adjusted until the desired output was attained. The sensing thermocouple, which was connected to the temperature controller, was equipped with a series cold junction continually immersed in an ice bath for maintenance of constant reactor temperature independent of changes in room temperature. The temperature in the thermocouple well of the

reactor was always 4-6°C below that of the annular space between the furnace wall and the reactor. It was felt that the thermocouple well temperature was more representative of the "true" reactor temperature and was used exclusively for subsequent calculations. Temperature cycling never exceeded ±1°C. This relatively high consistency resulted from having placed the controller sensor in the annular space between the furnace wall and the reactor which enhanced controller sensitivity. In addition, only 25 per cent of the power was obtained from the controller heater; thus, thermal inertia effects were minimized.

At each newly established temperature the reactor was conditioned in order to suppress heterogeneous components of the reaction[9]. Conditioning, which consisted of coating the walls of the reactor with a fine carbonaceous film formed from the pyrolysis of the reacting species, was accomplished by injecting a least 1 ml of acetonitrile under approximately the conditions of subsequent reactions. Though the heterogeneous processes were not studied per se, their effect was frequently observed in terms of enhancement of pyrolysis rate when reactor conditioning had not been thorough.

The carrier gas capillary flowmeter was calibrated with a "Precision" wet testmeter in terms of pressure drop (ΔP, cm) versus flow rate (data in Appendix B). Pressure drop was found to be a linear function of flow rate. Since the carrier gas flow rate was subject to changes resulting

from fluctuations in laboratory conditions i.e., temperature and pressure, correction was always made to insure maintenance of the desired molar flow rate. Ambient temperature was measured in the carrier gas stream immediately upstream from the flow meter and pressure downstream from the flow meter was assumed to be that of the laboratory which was measured with a mercury barometer. Under the conditions of run No. 1, ΔP was chosen to be 20.0 cm; thus, flow rate = 0.00554 (ΔP) = 0.1109 mmoles/sec.

Syringe injection rates were calibrated by injecting mercury into weighed vials (data in Appendix B). Using a 1.0 ml syringe, the following relationship was obtained:

drive potentiometer setting =
rate (mmoles of acetonitrile/sec) x 800

In the case of run No. 1, a concentration of 8 mole per cent acetonitrile was desired; thus, a flow rate of (0.1109)(0.08)/0.92 = 0.00963 mmole/sec of acetonitrile was needed; a potentiometer drive setting of 7.73 gave the desired concentration.

A material balance and trapping efficiency check was run on the flow system by simulating reaction conditions except that the reactor was at room temperature. Acetonitrile was injected into the carrier gas stream, trapped, and transferred to a cold finger. The amount of acetonitrile injected was known from the syringe cali-

bration data for the injection system and the time interval over which injection occurred. The amount of trapped acetonitrile was determined in two ways, (1) by weight of liquid in the cold finger and (2) by quantitative gas chromatographic analysis whereby the trapped acetonitrile was transferred to a cold finger containing a known weight of p-xylene standard (see Analytical Technique).

Having established the conditions to give the desired reactant concentration and contact time (which is determined by the total rate of flow), the following procedure was applied: Prior to connecting the needle to the flow apparatus, helium was allowed to flow through the entire system, including the trapping section, for about 5 minutes; this insured the removal of any previously deposited volatile material and flushed out oxygen. The acetonitrile to be used was degassed i.e., evacuated to remove dissolved air which would otherwise result in the formation of bubbles in the syringe during injection, thus displacing liquid volume. If this factor had been left unchecked, an error in the volume of acetonitrile injected would have resulted. After filling the syringe and affecting the removal of all air in the syringe and hypodermic needle, the injection system was assembled and inserted into the flow system. With the helium flow properly adjusted, the three-way stopcock, SC-3, was set so as to vent the system to the room. The syringe drive motor was actuated until it could be ascertained that the

syringe plunger had been displaced. This assured the removal of mechanical slack in the drive system. After 5 minutes of flushing and with all of the traps cooled with liquid nitrogen, stopcock, SC-3, was changed so as to direct the helium flow through the reactor; then, the syringe drive and an electric timer were actuated simultaneously. The tip of the hypodermic needle, from which acetonitrile was vaporizing, was carefully observed to insure that no liquid reactant was being injected into the gas stream; such an occurrence would lead to poorly defined concentrations. Adjustments of the power to the preheater section would eliminate such a problem. The partial pressure of acetonitrile was always maintained below its vapor pressure at room temperature. Following the injection of about 0.40 gm of acetonitrile, the syringe drive and timer were simultaneously stopped and the helium was allowed to flow for 5 minutes to carry all injected acetonitrile through to the trapping section. From a very precise syringe calibration curve, the amount of acetonitrile injected, to the nearest milligram, was determined. In the present case the injection time was 960 seconds, and 0.379 gm of acetonitrile was injected.

Having collected the pyrolysis products plus unreacted acetonitrile in the three "U" traps, the trapping section was isolated from the rest of the flow system, opened to the vacuum system, and evacuated to a pressure

of about 25 microns. One gram ($\pm$0.001 gram) of p-xylene standard was placed in a cold finger which then was connected to the vacuum system, frozen with liquid nitrogen, and evacuated along with the "U" traps. The p-xylene and reaction products were degassed to remove entrained gases which would otherwise reduce transfer efficiency. The vacuum pump was isolated from the vacuum system and the trap contents were transferred to the cold finger. When transfer was conplete, the resulting solution, containing a known amount of standard and unknown amounts of unreacted acetonitrile plus pyrolysis products, was ready for analysis to determine the amount of unreacted acetonitrile and the extent of reaction.

The extent of reaction was determined as follows:

amount acetonitrile injected = rate x time =
9.62×10^{-3} mmoles/sec x 0.041 gm/mmole x 960 sec = 0.379 gm

amount of unreacted acetonitrile =

0.730 (from calibration curves) x area ratio* =

$$0.730 \times 0.466 = 0.340 \text{ gm}$$

$$\text{per cent reaction} = \left(1 - \frac{0.340}{0.379}\right) \times 100 = 10.3$$

For experiments in which the reactant concentration was high i.e., 8 per cent, in calculating the contact time, a

*acetonitrile/p-xylene; see Analytical Technique section.

correction was made for volume change accompanying the reaction. It was assumed that on the average, pyrolysis of one mole of acetonitrile gave two moles of volatile product, thus a doubling of volume. Consequently, knowledge of the extent of reaction was needed for precise calculation of contact time. For the experiment under consideration, contact time was calculated as follows:

$$\text{extent of reaction} = 10.3 \text{ per cent}$$

$$\text{total flow at room temp.} = 0.1109 + 0.0096 + (0.103 \times 0.0096) = 0.1217 \text{ mmoles/sec}$$

assuming ideal gas behavior the molar volume at 880°C and 742 mm total pressure was

$$22.4 \times \frac{273 + 880}{273} \times \frac{760}{742} = 96.8 \text{ ml/mmole}$$

$$\text{contact time} = \frac{\text{reactor volume}}{\text{flow rate}} = \frac{73 \text{ ml}}{0.1217 \times 96.8} = 6.19 \text{ sec}$$

Materials

Eastman spectrograde acetonitrile, stored above Linde molecular sieves type 3A (for the adsorption of water) was used without further purification. Four ml portions sealed in vials were opened and degassed just prior to use. A mass spectrometric analysis showed very small peaks at mass numbers 18 and 28; all others could be accounted for by the acetonitrile spectrum and background. These peaks

probably resulted from trace amounts of water and nitrogen. From the magnitude of the ion peaks not accounted for by the acetonitrile spectrum, it was concluded the impurities amounted to less than one per cent.

Matheson, Coleman, and Bell analytical grade p-xylene was used as the internal standard for the quantitative gas chromatographic determination of acetonitrile.

Analytical Techniques

At the outset of the program it was believed that it would be possible to follow the reaction by some wet technique which would allow determination of cyanide ion, assuming the following stoichiometry:

$$CH_3CN \xrightarrow{\text{pyrolysis}} HCN + \text{other products}$$

Such a technique would permit direct calculation of product concentrations without having to rely on values determined by the difference in reactant concentrations. Since the latter method involves the determination of a relatively small number corresponding to the difference between two large numbers, inherent uncertainty is high.

It was subsequently found that about one-third (but not consistently) of the CN produced by the reaction remained in the system as a portion of the non-volatile polymeric residue therefore invalidating this method for determining the extent of reaction. Though this tech-

nique produced negative results in this investigation, the method is discussed in Appendix D.

The volatile products and reactant were analyzed quantitatively with an F and M, model 760, gas chromatograph equipped with a disc integrator. The sample and reference columns were 24 inches long, $\frac{1}{4}$ inch diameter stainless steel tubes and packed with 12 per cent diethylene glycol succinate on Johns-Manville Chromosorb W. A calibration curve was constructed by plotting several known weight ratios of acetonitrile to p-xylene against the area ratio obtained from the gas chromatographic peaks using 2 microliter injections (data in Appendix B). From the measured area ratios of acetonitrile to p-xylene and the calibration curve, the amount of unreacted acetonitrile was obtained. The selection of p-xylene as an internal standard was based on its resolvability with acetonitrile and hydrogen cyanide and upon its ability to produce moderately broad peaks. Pyrolysis products other than hydrogen cyanide never appeared on the gas chromatograms. With this system the maximum resolution of acetonitrile and p-xylene (columns at 50°C and carrier gas flow at 30 ml/min) was about 99 per cent. In addition, hydrogen cyanide, which had the shortest retention time, was virtually resolved from the acetonitrile.

The molar ratio of HCN/CH_4 in the reactor's exit stream was determined with a gas chromatograph which was

linked to the flow system by a Beckman gas sampling valve. The sample column ($2\frac{1}{2}$ ft x $\frac{1}{4}$ in) had 10 per cent dinonyl phthlate on Chromosorb W. The detector cell (homemade) was equipped with thermistors which were connected to a Wheatstone bridge. The output was registered on a Sargent recorder.

Mass spectrometer data were obtained with an Atlas mass spectrometer through the courtesy of The Upjohn Company.

Sample Calculation

The rate of chemical reaction of order n is defined as:

$$\text{rate} = -dc/dt = kc^n$$

For a stirred-flow reactor where it is assumed that the concentrations of reactant and products are uniform throughout and are representable by those in the exit stream,

$$\text{rate} = r = X/t = k(c_o - X)^n = k(1 - X/c_o)^n c_o^n$$

where X = change in concentration of reactant $(c_o - c)$,

c_o = initial concentration of reactant

c = concentration of reactant at time, t

X/c_o = fraction decomposed

t = contact time, reactor volume/volume rate of flow

Again, the results from run No. 1 are cited and the

reaction rate was calculated as follows:

extent of reaction = 10.3 per cent

initial concentration = 8 mole per cent of acetonitrile in the gas stream

molar volume (previously calculated) = 96.8 ml/mmole

contact time (previously calculated) = 6.19 sec

total flow rate (previously calculated) = 0.1217 mmoles/sec

thus,

total flow rate (previously calculated) = 0.1217 mmoles/sec or $0.1217 \times 96.8 = 11.8$ ml/sec

initial concentration = $c_o = 0.1217 \times 0.08/11.8 = 0.824 \times 10^{-3}$ or 0.824 mmoles/lit

change in concentration = $X = 0.824 \times 0.103 =$ 0.085 mmoles/lit

hence,

$r = X/t = 0.085/6.19 = 0.0137$ mmoles lit^{-1} sec^{-1} = $k(0.824 - 0.085)^n = k(0.739)^n$

The order of the reaction, n, was obtained from the slope of a graph of log c versus log r. The best value

of n obtained from the data at each temperature was about 1.2. Thus, it appeared that the rate had to be represented by a more complex expression.

Plots of r/c versus c yielded straight lines whose y intercepts and slopes gave first and second order rate constants respectively.

RESULTS AND DISCUSSION

Reaction Products

All peaks (minus background) which appeared in the mass spectrum of the exit gases along with the species to which they were attributed are shown in Table I.

TABLE I
Mass Spectrometer Data

mass No.	relative peak height at 10% decomp.	at 60% decomp.	probable specie(s)
15	4	16	CH_3
16	4	21	CH_4
26	2	7	CN, C_2H_2
27	9	45	HCN, C_2H_3
28	8	3	C_2H_4
38	8	1	CCN
39	15	3	CHCN
40	43	10	CH_2CN
41	85	20	CH_3CN
51	0.5	1	CCHCN, CHCCN
52	0.5	1	CHCHCN, CH_2CCN
53	0.5	1	CH_2CHCN

The major volatile products of the thermal decomposition of acetonitrile were hydrogen cyanide and methane. Unlike previously reported results[1] on the pyrolysis of acetonitrile at 865°C, hydrogen did not appear in detectable quantities. Ethane also was not observed as a reaction product. The formation of these products was not expected since it probably would have involved highly improbable third body collisions. Compared to the major volatile products, C_2H_4 (28) and CH_2CHCN (53) appeared only in relatively small amounts.

A brown, non-volatile, polymeric material formed by the reaction coated the walls of the reactor outlet and the cold traps. This residue was readily soluble in acetone and dimethylsulfoxide. Quantitative elemental analysis of the residue (57.7%C, 3.18%H, 31.5%N) suggested the following emperical formula: $(C_{11}H_7N_5)_n$. The infrared spectrum showed major absorption at 2200 cm^{-1} which roughly corresponds to the CN stretch. A network cyclic structure has been suggested as a possible product resulting from the polymerization of cyanogen[10]; however, these authors suggested that this material is unstable at temperatures above 850°C. It is therefore felt that the average structural unit for the polymeric residue is of the form:

$$(CHCN\text{-}CHCN\text{-}CHCN\text{-}CH_2\text{-}CHCN\text{-}CHCN)_n$$

This material could have formed in the reactor's exit from fragments of molecules or radicals.

Kinetic Results

The results produced by flow experiments are illustrated in Figures 3 through 10 and the data are shown in tabular form in Appendix A. Figures 3 through 6 show the fraction of acetonitrile decomposed, X/c_o (where X is the change in acetonitrile concentration resulting from decomposition and c_o is the initial concentration

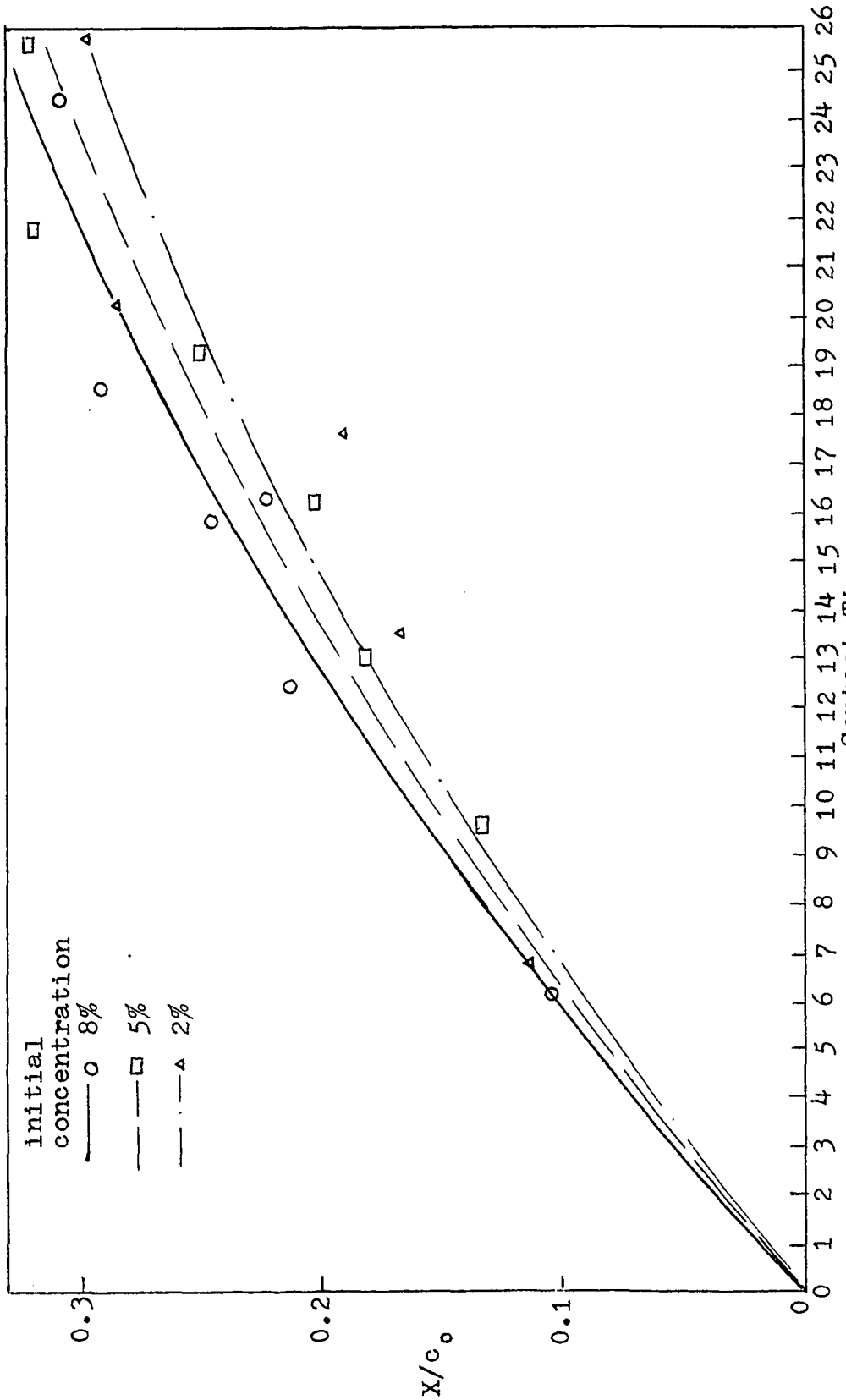

Figure 3 Extent of Reaction versus Contact Time at 880°C.

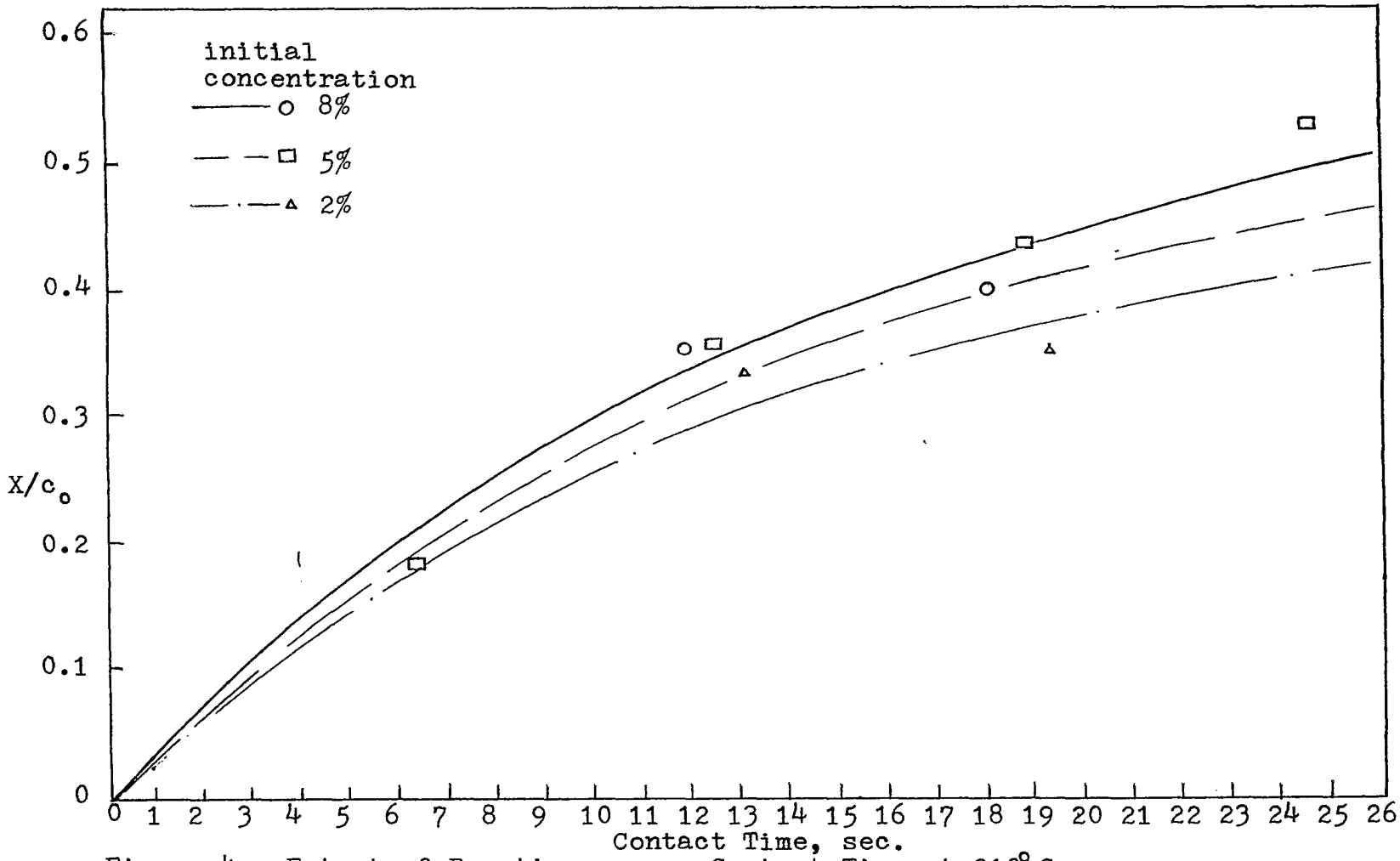

Figure 4 Extent of Reaction versus Contact Time at 910° C.

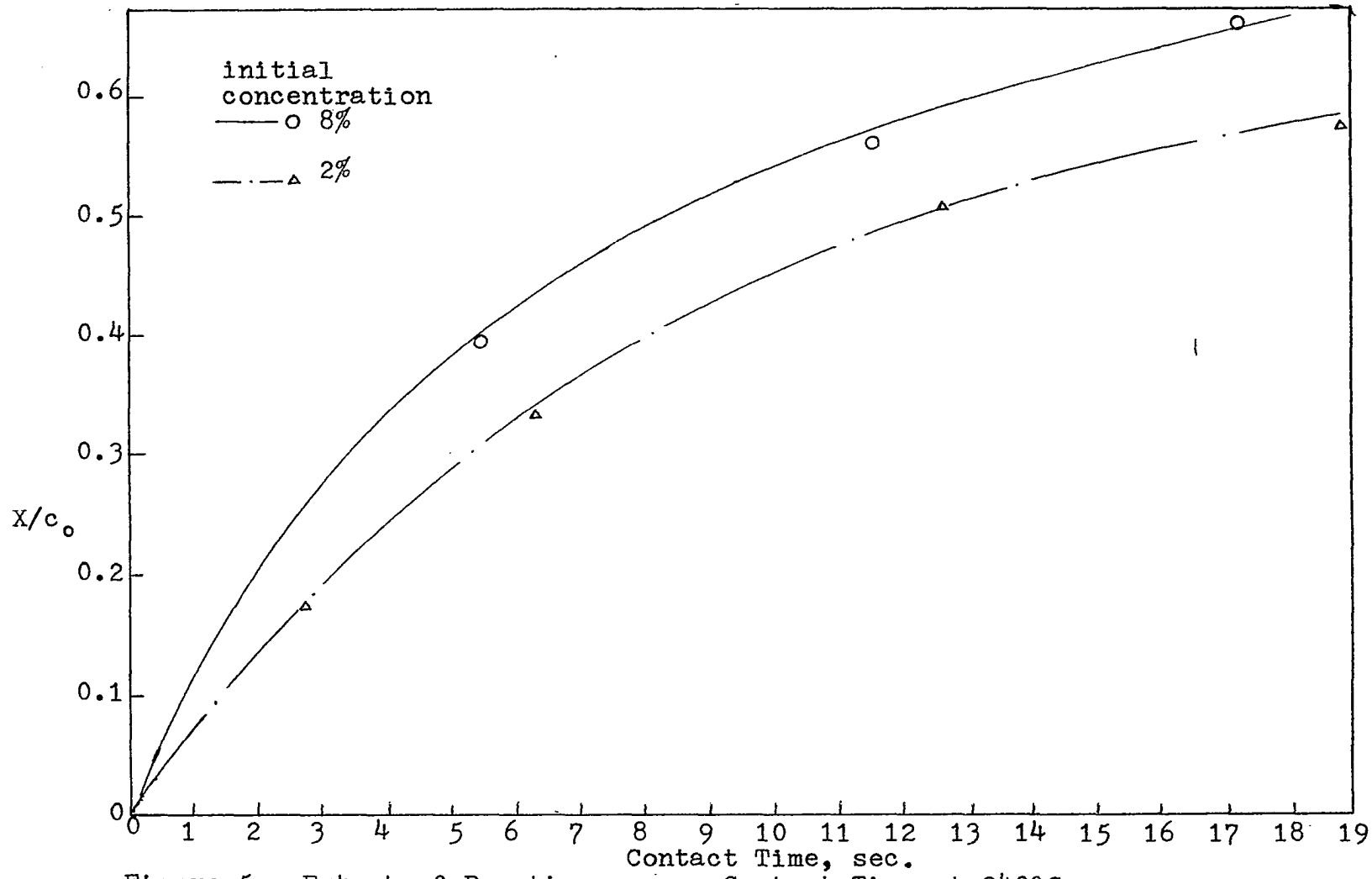

Figure 5 Extent of Reaction versus Contact Time at 940°C.

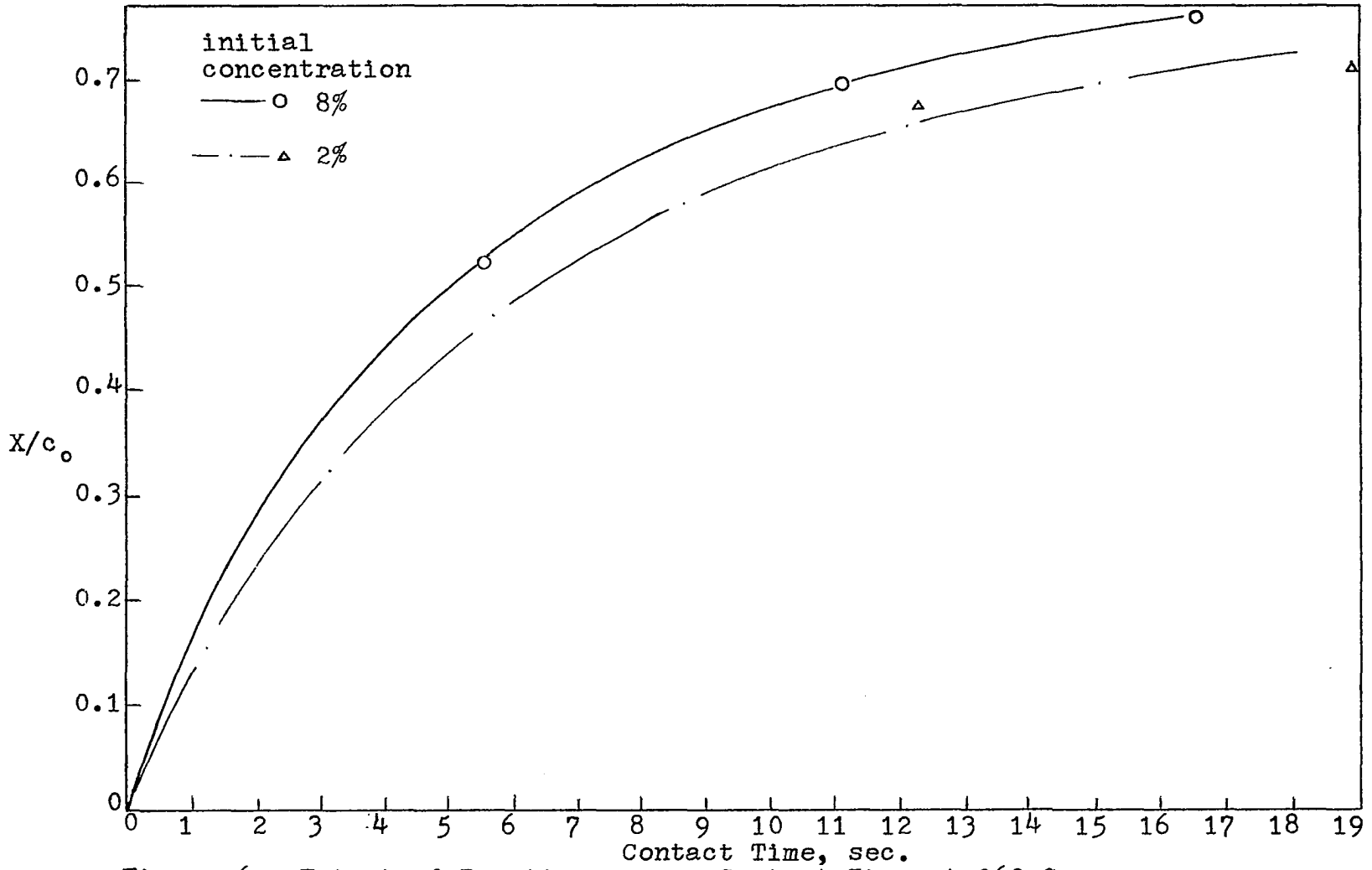

Figure 6 Extent of Reaction versus Contact Time at 960_oC.

of acetonitrile) as a function of contact time and initial concentration at 880, 910, 940, and 960°C respectively.

It was found that the rate expression which best fit the data was of the form:

$$r = X/t = k_1(c_o - X) + k_2(c_o - X)^2$$

where k_1 and k_2 = first and second order specific rate constants

r = rate, mmoles lit^{-1} sec^{-1}

X = change in reactant concentration, mmoles lit^{-1}

$(c_o - X)$ = acetonitrile concentration in the reactor, mmoles lit^{-1}

The curves in Figures 3 through 6 were obtained from the differential form of the rate equation, e.g., for a given c_o and per cent reaction the corresponding contact time can be calculated using the rate constants for that temperature. It is necessary to use this approach when calculating concentration versus time curves for stirred-flow reactors. On the other hand, it is necessary to use the integrated form of the rate equation when dealing with concentration versus time data from tubular flow reactors or static systems. The differential rate equation can be integrated as follows:

$$-dc/dt = k_1c + k_2c^2$$

$$-\frac{dc}{c(k_1 + k_2c)} = dt$$

$$\frac{1}{k_1}\ln\frac{k_1 + k_2c}{c} + \text{constant} = t$$

when $t = 0 \quad c = c_o$

therefore $\text{constant} = -\frac{1}{k_1}\ln\frac{k_1 + k_2c_o}{c_o}$

and $\frac{1}{k_1}\ln\frac{k_1 + k_2c}{c}\cdot\frac{c_o}{k_1 + k_2c_o} = t$

or $\frac{c_o(k_1 + k_2c)}{c(k_1 + k_2c_o)} = \exp(k_1t)$

The rate constants, k_1 and k_2, were determined from the least square intercept and slope represented by the following equation and are presented in Table II:

$$\frac{r}{(c_o - X)} = k_1 + k_2(c_o - X)$$

Plots of $r/(c_o - X)$ versus $(c_o - X)$ at the four operating temperatures are shown in Figures 7 and 8. Uncertainties in the individual measurements and their effect on the end results are given in Appendix C. Analyses of Arrhenius plots (Figures 9 and 10) of the first and second-order rate constants lead to the following expressions for the rate constants:

$$k_1 = 10^{11.8}\exp(-72{,}000\pm3{,}700)/RT \ (\text{sec}^{-1})$$

$$k_2 = 10^{20.5}\exp(-120{,}000\pm6{,}200)/RT \ (\text{lit. mmole}^{-1}\ \text{sec}^{-1})$$

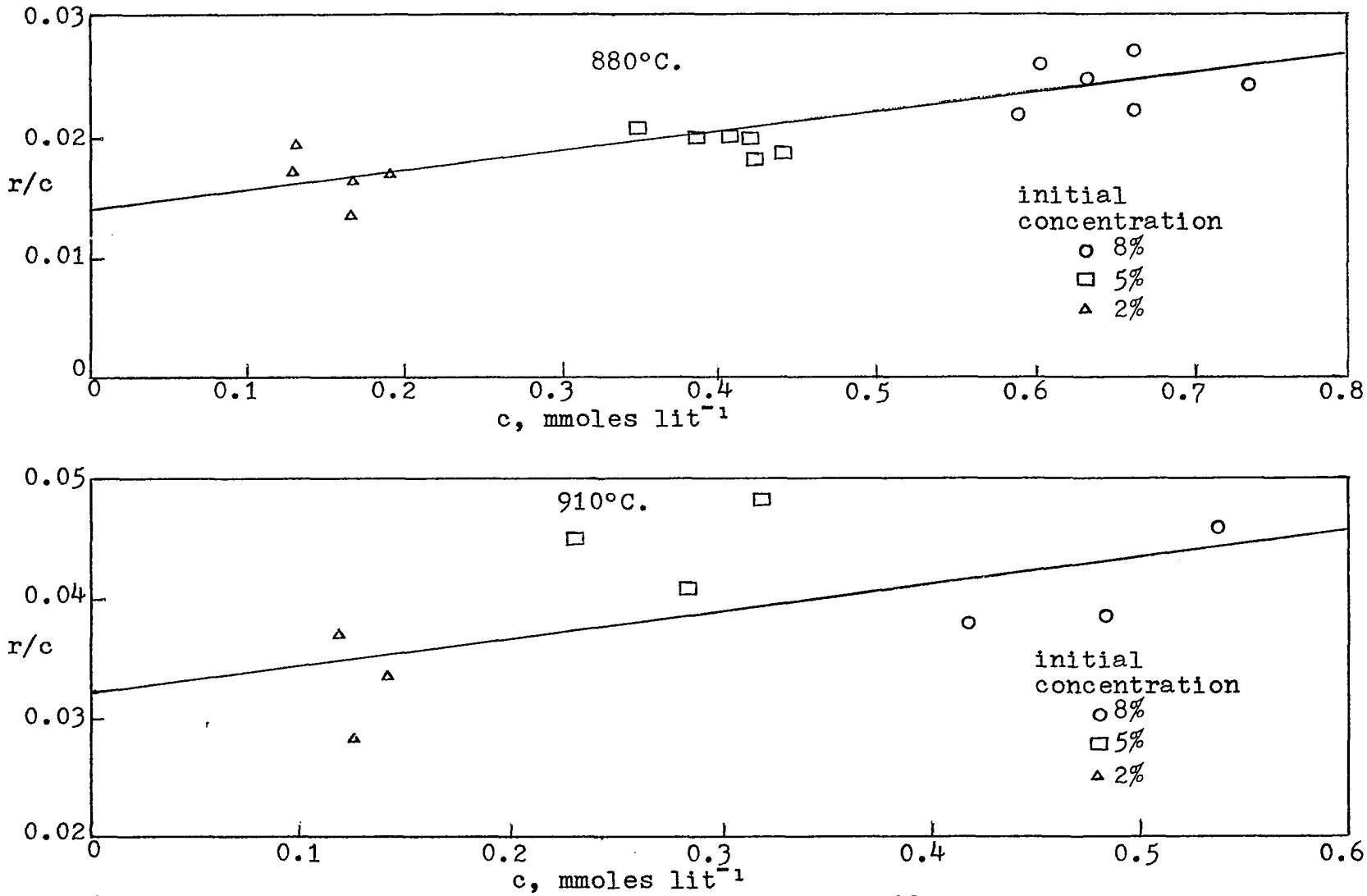

Figure 7 First -second order plot of rate data at 880 and 910°C.

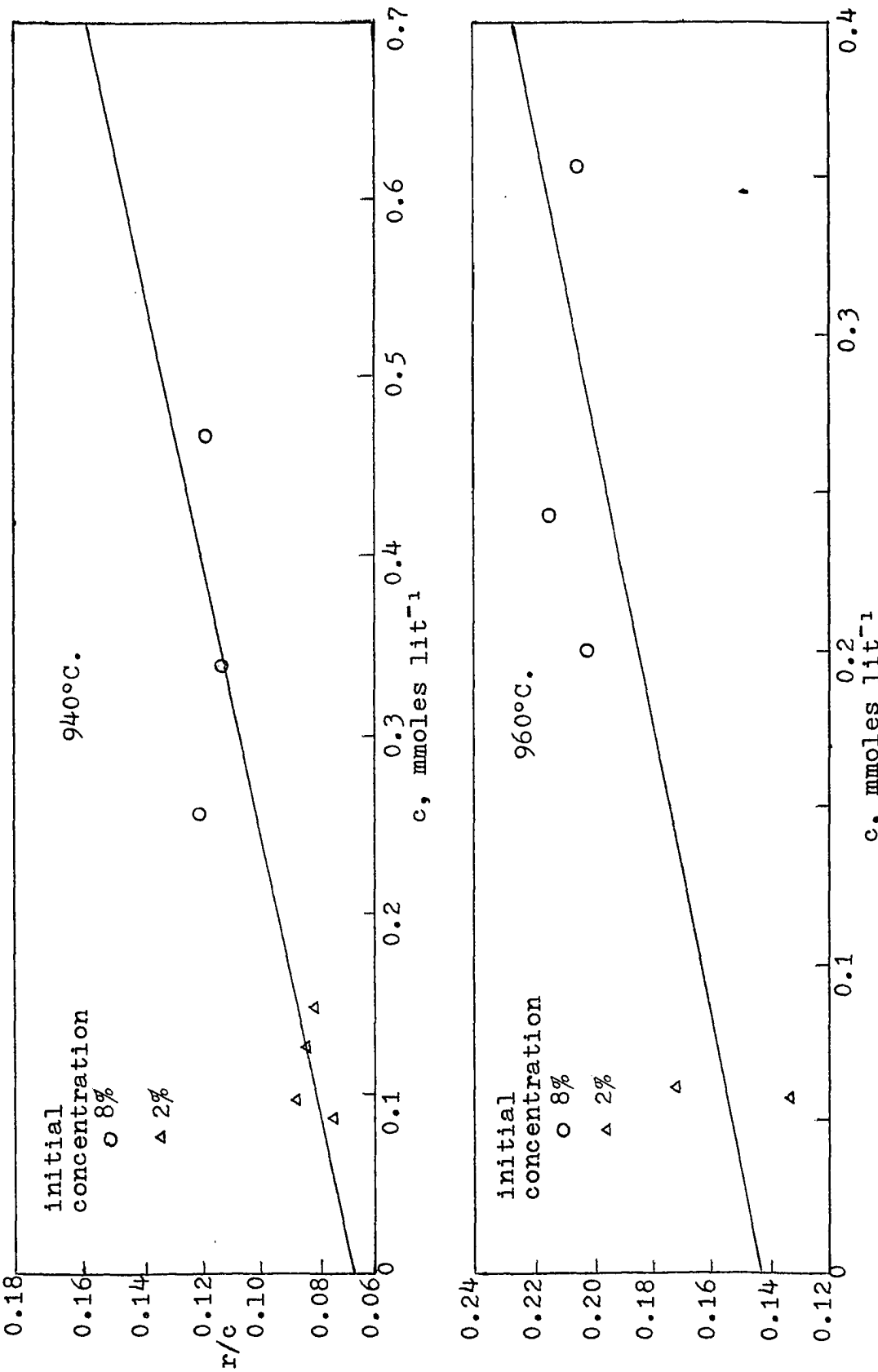

Figure 8 First-second order plot of rate data at 940 and 960°C.

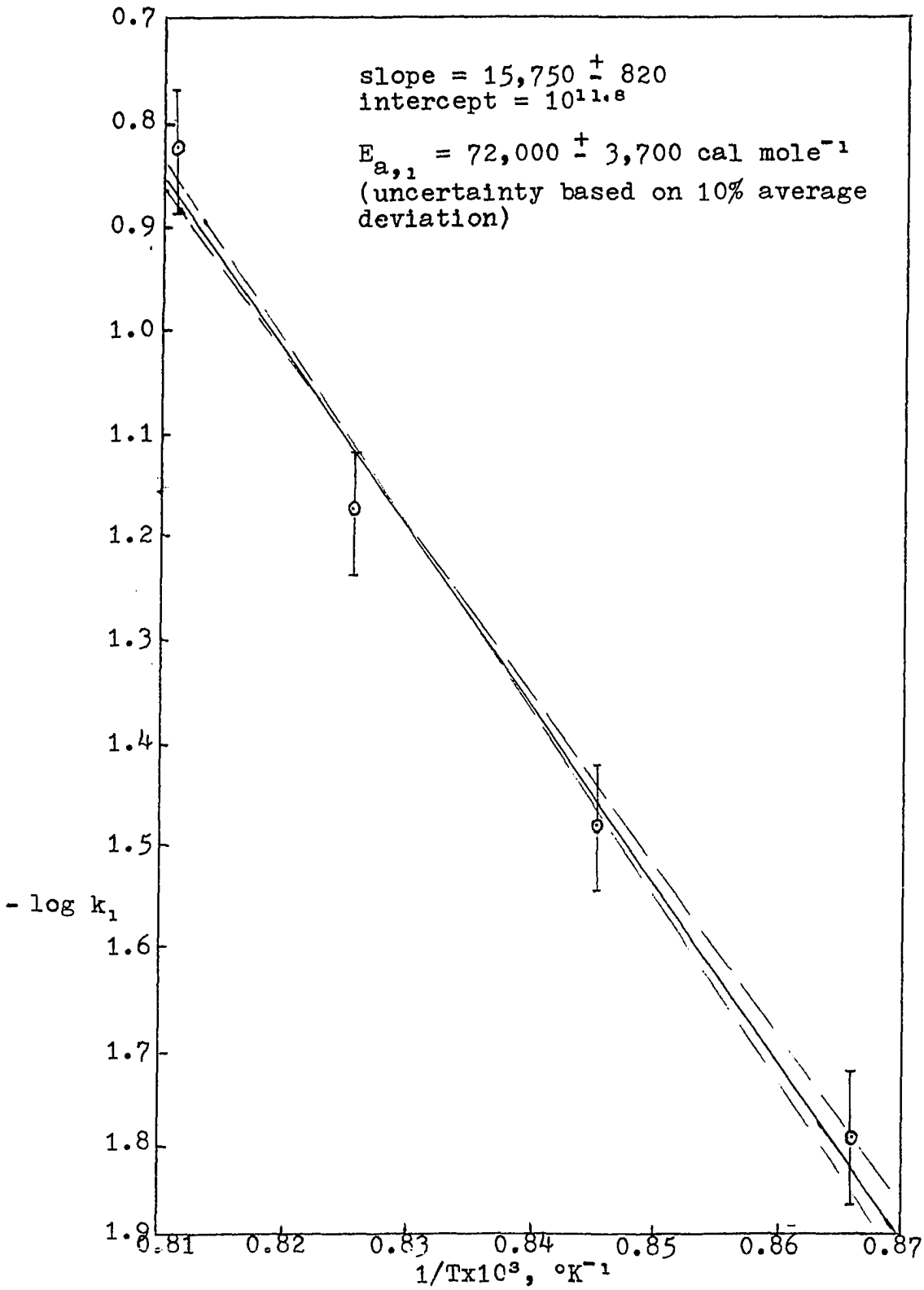

Figure 9 Arrhenius Plot (first-order rate constants)

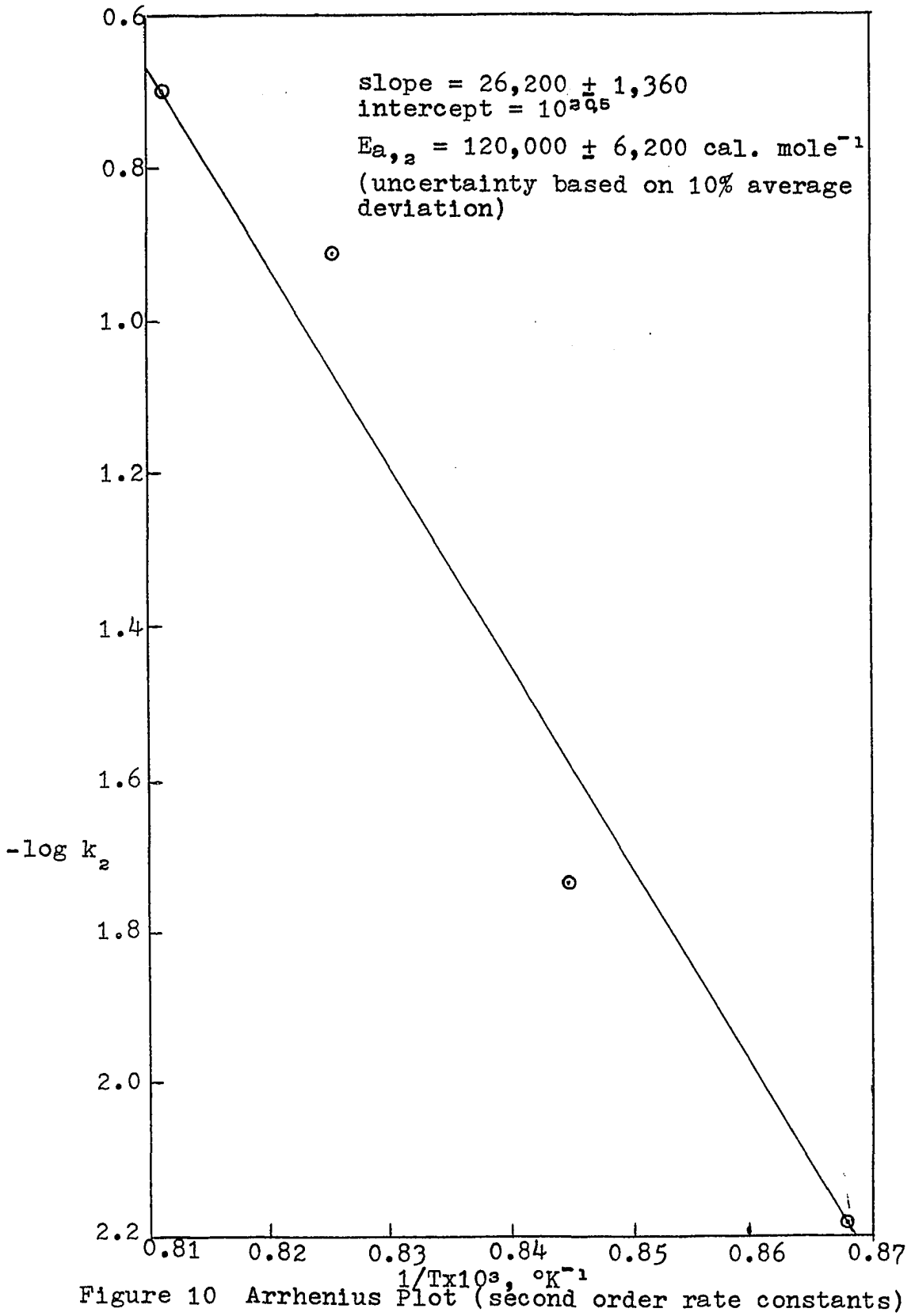

Figure 10 Arrhenius Plot (second order rate constants)

TABLE II

Kinetic Results

T °K	$1/T \times 10^3$	k_1 sec^{-1}	k_2 $lit\ mmole^{-1}\ sec^{-1}$	$-\log k_1$	$-\log k_2$
1153	0.867	0.015	0.0064	1.796	2.194
1183	0.845	0.033	0.019	1.481	1.721
1213	0.825	0.067	0.126	1.174	0.900
1233	0.811	0.146	0.198	0.836	0.703

Calculation of the CH_3-CN Bond Energy

Using the most recent thermodynamic data[11], the bond dissociation energy for the carbon-carbon bond in acetonitrile at 907°C was calculated as 115.5 kcal/mole whereas 103 kcal/mole is reported using the electron impact technique[12]. The former value is known to have large uncertainty and the applicability of the latter at a given temperature is questionable. The activation energy for the first order term was determined to fall within the range 68-76 kcal/mole. The fact that the carbon-carbon and the carbon-hydrogen bond energies are significantly higher than the observed activation energy for the overall reaction is evidence of the radical chain nature of the reaction. The lower C-H bond energy (95-100 kcal/mole) suggests the possibility that the rupture of this bond is the primary initiation step.

Quantitative Analysis of Products

Several subsequent runs were made using a flow system similar to the one described earlier, except that samples of the gaseous products plus acetonitrile were taken di-

rectly from the reactor's exit stream and fed into an on-stream gas chromatograph. A shift in the relative amounts of the major products, i.e., hydrogen cyanide and methane, was observed and the shift was found to be a function of extent of reaction and not of temperature. From the peak area ratios and relative response factors*, the molar ratio, HCN/CH_4, was found to range from about 1.5 at 50 per cent decomposition to about 0.5 at 5 per cent decomposition (see Appendix A).

Reaction Mechanism

An acceptable mechanism must be able to account for

1) the origin of all observed products,

2) the observed rate law for the reaction, i.e., $-d(CH_3CN)/dt = k_1(CH_3CN) + k_2(CH_3CN)^2$,

3) the shift in major products with extent of reaction, and reconcile,

4) the low activation energy associated with the first-order rate constant and the high carbon-carbon bond energy ($E_{a,1}$ = 72.0 kcal and ΔH_{CH_3-CN} = 115.5 kcal*),

*A relative response factor for hydrogen cyanide was not available from the literature and therefore was estimated to be 50 (relative to benzene = 100) by extrapolation to molecular weight 27 on a plot of molecular weight versus relative response factor for the alkyl nitrile homologous series. Values for the higher alkyl nitriles were obtained from ref. (13).

5) the comparable magnitudes of the activation energy associated with the second-order rate constant and the carbon-carbon bond energy ($E_{a,2}$ = 120.0 kcal and ΔH_{CH_3-CN} = 115.5 kcal*).

A mechanism that meets the requirements for the first-order term is as follows (steps 2c, 3b, and 4b have been omitted from the steady-state treatment for reasons to be discussed later):

initiation: $CH_3CN \xrightarrow{1a} H + CH_2CN$

$CH_3CN \xrightarrow{1b} CH_3 + CN$

propagation: $H + CH_3CN \xrightarrow{2a} HCN + CH_3$

$CH_3 + CH_3CN \xrightarrow{2b} CH_4 + CH_2CN$

$CN + CH_3CN \xrightarrow{2c} HCN + CH_2CN$

$CH_2CN \xrightarrow{3a} H + CHCN$

$CH_2CN \xrightarrow{3b} CH_2 + CN$

termination: (first-order) $CH_3 + CH_2CN \xrightarrow{4a} C_2H_4 + HCN$

$H + CH_2CN \xrightarrow{4b} CH_2 + HCN$

Methylene (CH_2) may lead to the formation of CH_4 by abstracting a hydrogen atom from acetonitrile or may dimerize

*This value was considered to be more reliable at reaction temperatures than the value determined by the electrom impact technique.

to form ethylene (C_2H_4). This latter process is believed to be of little importance due to the observation of only trace amounts of ethylene in the mass spectra. The polymeric residue and higher nitriles are believed to form by the following processes:

$$n(CHCN) \longrightarrow \text{polymers}$$

$$CHCN + CH_3 \longrightarrow CH_2CHCN + H$$

$$CHCN + CH_2CN \longrightarrow CH_2CHCN + CN$$

$$CH_2 + CH_3CN \longrightarrow C_2H_4 + HCN$$

$$CH_2 + CH_3CN \longrightarrow CH_3 + CH_2CN$$

$$CHCN + HCN \longrightarrow \text{polymers}$$

$$\text{polymers} \longrightarrow HCN \text{ (or } CN) + \text{polymers}'$$

The steady-state treatment of the Rice-Herzfeld[14] first-order mechanism is as follows (steps 1-4):

$$d(CH_3)/dt = 0 = -k_{2b}(CH_3)(CH_3CN) + k_{2a}(H)(CH_3CN) - k_{4a}(CH_3)(CH_2CN) + k_{1b}(CH_3CN) \quad (a)$$

$$d(H)/dt = 0 = -k_{2a}(H)(CH_3CN) + k_{3a}(CH_2CN) + k_{1a}(CH_3CN) \quad (b)$$

$$d(CH_2CN)/dt = 0 = k_{2b}(CH_3)(CH_3CN) - k_{4a}(CH_3)(CH_2CN) - k_{3a}(CH_2CN) + k_{1a}(CH_3CN) \quad (c)$$

$$\text{from (b)} \quad k_{1a}(CH_3CN) + k_{3a}(CH_2CN) = k_{2a}(H)(CH_3CN)$$

$$\text{or } (CH_2CN) = \frac{k_{2a}(H)(CH_3CN) - k_{1a}(CH_3CN)}{k_{3a}}$$

the summation of (a) and (c) gives

$$0 = k_{2a}(H)(CH_3CN) - 2k_{4a}(CH_3)(CH_2CN) + k_{1b}(CH_3CN) - k_{3a}(CH_2CN) + k_{1a}(CH_3CN)$$

substitution for $k_{3a}(CH_2CN)$ from above gives

$$0 = 2k_{4a}(CH_3)(CH_2CN) - k_{1b}(CH_3CN) - 2k_{1a}(CH_3CN)$$

If it is assumed that step 1b is insignificant compared to 1a i.e., $2k_{1a} \gg k_{1b}$, then

$$k_{4a}(CH_3)(CH_2CN) = k_{1a}(CH_3CN)$$

$$(CH_3) = \frac{k_{1a}(CH_3CN)}{k_{4a}(CH_2CN)}$$

substitution of (CH_2CN) from above and assumption that $k_{2a}(H) \gg k_{1a}$ (necessary for radical chain mechanism)

$$(CH_3) = \frac{k_{1a}(CH_3CN)}{k_{4a}k_{2a}(H)(CH_3CN)/k_{3a}} = \frac{k_{1a}k_{3a}}{k_{4a}k_{2a}(H)}$$

insertion of (CH_3) and (CH_2CN) into (c) leads to

$$0 = \frac{k_{2b}k_{1a}k_{3a}(CH_3CN)}{k_{4a}k_{2a}(H)} - \frac{k_{4a}k_{1a}k_{3a}}{k_{4a}k_{2a}(H)} \cdot \frac{k_{2a}(H)(CH_3CN)}{k_{3a}} - k_{2a}(H)(CH_3CN) + k_{1a}(CH_3CN)$$

$$0 = \frac{k_{2b}k_{1a}k_{3a}}{k_{4a}k_{2a}(H)} - k_{1a} - k_{2a}(H) + k_{1a}$$

$$k_{2a}^2(H)^2 = \frac{k_{2b}k_{1a}k_{3a}}{k_{4a}}$$

therefore

$$(CH_3) = \frac{k_{1a}k_{3a}}{k_{4a}k_{2a}(H)} = \frac{k_{1a}k_{3a}}{k_{4a}(k_{2b}k_{1a}k_{3a}/k_{4a})^{1/2}} = \left(\frac{k_{1a}k_{3a}}{k_{4a}k_{2b}}\right)^{1/2}$$

For the overall reaction

$$\text{rate} = -d(CH_3CN)/dt = k_{2a}(H)(CH_3CN) + k_{2b}(CH_3)(CH_3CN)$$

k_{1a} assumed small compared to $k_{2a}(H)$ as before

$$\text{rate} = \left(\frac{k_{2b}k_{1a}k_{3a}}{k_{4a}}\right)^{1/2}(CH_3CN) + k_{2b}\left(\frac{k_{1a}k_{3a}}{k_{4a}k_{2b}}\right)^{1/2}(CH_3CN) = 2\left(\frac{k_{2b}k_{1a}k_{3a}}{k_{4a}}\right)^{1/2}(CH_3CN)$$

which leads to an expression for the theoretical activation energy

$$E_a = 1/2(E_{1a} + E_{2b} + E_{3a} - E_{4a})$$

If step 4b were used as a termination process and k_{4b} were substituted for k_{4a}, an identical rate expression would be obtained.

The assumption regarding the initiation process i.e., 1a>>1b, where H and CH_2CN are the preferred products was made because of the relative bond energies (ΔH_{H-CH_2CN} = 95-100 kcal and ΔH_{CH_3-CN} = 115.5 kcal) and was reinforced by the photolysis results of previous investigators[2]. As a consequence of the above assumption step 2c was considered negligible due to the low concentration of CN. Step 3b was not considered because of the relative bond energies i.e., C-C > C-H. (Supporting this argument is the observation

that the ion fragment peaks of the mass spectra of acetonitrile show that all of the hydrogens are stripped from the methyl carbon much more readily than is the carbon-carbon bond broken.)

The following process must be considered most unfavorable on theoretical grounds[2] i.e., shielding, though it has been invoked on occasions:

$$H + CH_3CN \longrightarrow CH_4 + CN$$

The observed shift in products (the ratio HCN/CH_4 increased as extent of reaction increased) can only be explained in terms of the relative amounts of CN which appeared in the polymeric residue (data in Appendix A).

If it is assumed that the activation energies for steps 1a, 2b, 3a, and 4a are 95-100, 5-10, 45-55*, and 0.5-1.0 kcal/mole respectively, a theroreical activation energy of 72-82 kcal/mole is obtained. Values in this range are relatively consistent with the observed first order activation energy of 72 kcal/mole. This result adds considerable support to the arguments thus far proposed.

To satisfy the requirements imposed by the kinetic data, a second order reaction has been proposed; the mech-

---

*This range of values was estimated on the basis of the relative stability of the carbene resulting from the process compared to that of the starting radical.

anistic detail for such a reaction path is highly speculative.

$$2CH_3CN \longrightarrow [\text{activated complex}] \longrightarrow \text{products}$$

The three-halves order radical chain mechanism (by second order initiation or alternate termination steps) was investigated as a possibility for the present problem; however, this approach lead to the prediction of a much lower activation energy than that which was observed (120 kcal). This activation energy is of the order of the carbon-carbon bond energy at the reaction temperatures, 115.5 kcal.

Several approaches involving consecutive reaction schemes were considered; however, these did not yield the observed concentration dependence, thus were discarded. Inclusion of second order kinetics seemed to be the only means of reconciling the high activation energy of the second term in the observed kinetic data.

APPENDIX A

Kinetic Data

Symbols:

c_o = initial concentration of acetonitrile (mmoles lit^{-1})

t = contact time (sec)

X = concentration of acetonitrile reacted (mmoles lit^{-1})

X/c_o = fraction of acetonitrile decomposed

c = concentration of acetonitrile

conc. = mole per cent of acetonitrile in helium

$X/t = r$ = rate (mmoles lit^{-1} sec^{-1})

Data at 880°C (1153°K)

run no.	conc.	c_o	t	X/c_o	X/t	c	r/c
1	8	0.824	6.2	0.103	0.0137	0.739	0.0185
2	2	0.219	6.7	0.116	0.0031	0.193	0.0159
3	2	0.206	13.4	0.171	0.0026	0.171	0.0153
4	5	0.500	12.9	0.182	0.0071	0.409	0.0173
5	8	0.825	12.4	0.215	0.0143	0.648	0.0221
6	2	0.206	20.2	0.285	0.0029	0.147	0.0199
7	5	0.516	19.2	0.250	0.0067	0.387	0.0174
8	8	0.832	18.5	0.290	0.0131	0.590	0.0222
9	2	0.206	26.5	0.300	0.0023	0.144	0.0163
10	8	0.822	24.5	0.308	0.0103	0.569	0.0181
11	5	0.515	25.5	0.325	0.0066	0.348	0.0188
12	5	0.516	9.5	0.136	0.0073	0.446	0.0164
13	5	0.516	16.2	0.203	0.0065	0.411	0.0157
14	5	0.516	21.7	0.325	0.0077	0.348	0.0222
15	8	0.820	16.2	0.217	0.0109	0.642	0.0170
16	2	0.205	17.6	0.188	0.0022	0.166	0.0134
17	8	0.820	15.8	0.246	0.0127	0.619	0.0205

Data at 910°C (1183°K)

run no.	conc.	c_o	t	X/c_o	X/t	c	r/c
18	5	0.500	6.3	0.188	0.0150	0.406	0.0369
19	2	0.200	6.5	0.174	0.0054	0.165	0.0325
20	2	0.201	13.0	0.330	0.0051	0.135	0.0278
21	5	0.505	12.3	0.361	0.0148	0.323	0.0458
22	8	0.808	11.9	0.345	0.0234	0.529	0.0443
23	8	0.807	17.9	0.399	0.0180	0.485	0.0371
24	5	0.506	18.7	0.434	0.0117	0.287	0.0407
25	2	0.202	19.2	0.352	0.0037	0.131	0.0282
26	5	0.503	24.5	0.526	0.0108	0.238	0.0454

Data at 940°C (1213°K)

run no.	conc.	c_o	t	X/c_o	X/t	c	r/c
27	2	0.196	6.3	0.333	0.0106	0.130	0.0815
28	8	0.785	5.7	0.404	0.0556	0.468	0.1190
29	2	0.196	12.5	0.504	0.0079	0.097	0.0813
30	8	0.782	11.4	0.561	0.0385	0.343	0.1120
31	2	0.196	18.7	0.574	0.0061	0.083	0.0730
32	8	0.790	17.1	0.664	0.0306	0.266	0.1150
33	2	0.177	2.6	0.177	0.0119	0.146	0.0815

Data at 960°C (1233°K)

run no.	conc.	c_o	t	X/c_o	X/t	c	r/c
34	8	0.770	5.6	0.527	0.0732	0.364	0.201
35	2	0.192	12.3	0.676	0.0106	0.062	0.171
36	8	0.778	11.1	0.700	0.0489	0.232	0.211
37	8	0.776	16.6	0.765	0.0358	0.182	0.197
38	2	0.192	19.0	0.710	0.0072	0.056	0.128

Data From Quantitative Analysis of Products

temp.	conc.	t	X/c_o	peak area ratio	molar ratio HCN/CH_4
967	5.3	6.0	0.52	2.07	1.48
967	1.9	2.3	0.24	1.55	1.11
880	5.6	4.6	0.09	0.90	0.65
981	1.9	1.3	0.18	1.07	0.77
982	2.0	6.5	0.52	1.97	1.31
902	2.9	10.4	0.15	1.24	0.89
930	1.9	1.5	0.06	0.75	0.53
931	1.7	4.1	0.20	1.23	0.88

APPENDIX B

Calibration Data

Helium Flow Rate--small capillary (0.5 mm x 6 cm)

pressure drop, cm	flow rate, mmoles/sec
24.1	0.134
19.7	0.109
15.7	0.086
11.4	0.063
8.2	0.045
3.8	0.021

thus, flow rate = $(0.000554)(\Delta P)$ at 25°C and 740 mm Hg total pressure

Rate of Injection

syringe drive potentiometer setting	rate of injection x 10^4 ml/sec
1.00	0.67
3.00	1.97
5.00	3.32
7.00	4.62
9.00	5.92

thus, injection rate (ml/sec of acetonitrile) =

$$(0.000065)(\text{setting})$$

The molar and weight flow rates were calculated using 41.05 gms/mole and 0.785 gm/ml[15] as the molecular weight and density of acetonitrile respectively. The temperature at the syringe during any given run was 25 $\pm$ 2°C; this relative consistency resulted from the close proximity of the syringe to the furnace, thus reducing the

magnitude of normal room temperature fluctuations.

Gas Chromatographic Analysis--weight and area ratios of acetonitrile to p-xylene

weight ratio, acetonitrile/p-xylene	area ratio acetonitrile/p-xylene
0.100	0.135
0.200	0.270
0.300	0.405
0.400	0.545

thus, weight of acetonitrile/gm p-xylene = (0.735)(area ratio)

APPENDIX C

Analysis of Uncertainties

Uncertainties for individual measurements and their influence on the final results were estimated in the following manner:

1) The uncertainty in the helium flow rate depended upon the magnitude of the pressure drop which could be read to $\pm$0.1 cm. The lowest and highest readings were 5.0 cm and 20.0 cm respectively. Thus, the maximum and minimum uncertainties were 0.1/5.0 = 2.0% and 0.1/20.0 = 0.5%. Maximum uncertainty, therefore, occurred at long contact times.

2) Uncertainty in the amount of acetonitrile injected was based on the injection rate. The limit of reproducibility determined the uncertainty in injection rate which was felt to be about $\pm$0.001 microliters/sec. Thus, the largest uncertainty occurred at the lowest concentration (2%) and the longest contact time where the rate was 0.04 microliters/sec and was 2.5%. The smallest uncertainty was about 0.2% when the injection rate was 0.5 microliters/sec. Uncertainties in time measurements were considered negligible.

3) The volume of the reactor was measured to about

± 2 ml and the total volume was approximately 73 ml. Hence, the uncertainty was 2/73 = 2.7%. This source of uncertainty was not random and consequently did not contribute to the random behavior of the individual values, rather, was added to the final uncertainty in the rate constants. Due to the very low coefficient of thermal expansion of Vycor, volume changes accompanying temperature changes were considered negligible.

4) The uncertainty in the gas chromatographic determination of the amount of unreacted acetonitrile arose principally from random instrumental factors which resulted in irreproducibility. Typically, these uncertainties were 0.01/0.30 = 3.3%. Since all weighings were made with extreme caution i.e., ±0.5 mg, it was felt that the uncertainty arising from the preparation of the calibration samples never exceeded 1%.

5) Uncertainties in initial concentration arose from (1) and (2) while those in final concentration were related to (1), (2), and (4).

Uncertainty in initial concentration--

Maximum: 2.0% + 2.5% = 4.5%

Minimum: 0.5% + 0.2% = 0.7%

Uncertainty in final concentration--

Maximum: 2.0% + 2.5% + 3.3% = 7.8%

Minimum: 0.6% + 0.2% + 3.3% = 4.1%

6) Uncertainties in contact time resulted principally from those in the helium flow rate i.e., 0.5% to 2.0%. However, minor contributions result from uncertainties in the injection rate and changes in gas volume accompanying pyrolysis. This latter point was further complicated by the formation of non-volatile residues from the decomposition products. It was estimated that at short contact time and high concentrations, the uncertainty in the gas volume had its maximum value of 0.7% and 0.1% as its minimum value at long contact times and low concentrations. This source of uncertainty resulted from uncertainty in extent of reaction and from the fact that the formation of polymeric residue reduced the volume of gases.

Uncertainty in contact time--

Maximum: 2.0% + 0.7% = 2.7%

Minimum: 0.6% + 0.1% = 0.7%

Uncertainties in the reactor's volume contributes to the uncertainty in contact time; however, this has been discussed in (3).

7) Uncertainties in the rate constants depend on the total uncertainty in the difference between initial and final concentrations which is highly dependent on the extent of reaction. The following examples are illustrative:

(a) If the initial concentration (run No. 2) c_o = 0.219 mmoles/lit and the final concentration

$$c = 0.193 \text{ mmoles/lit}$$

$$t = 6.7 \text{ sec}$$

$$T = 880°C$$

Since the contact time is low (high flow rate), the minimum concentration uncertainty is applicable.

$$X = c_o - c = 0.219 \pm 0.219 \times 0.7\% - 0.193 \pm 0.193 \times 4.1\% =$$

$$(0.219 \pm 0.002) - (0.193 \pm 0.008) = 0.026 \pm 0.010$$

Therefore, the total uncertainty in X is $\pm 0.010/.026 = \pm 38\%$

(b) If the initial concentration (run No. 10) c_o = 0.822 mmoles/lit and the final concentration

$$c = 0.569 \text{ mmoles/lit}$$

$$t = 24.5 \text{ sec}$$

$$T = 880°C$$

Since the contact time is long, but the concentration high, an uncertainty value greater than minimum but less than maximum is applicable.

$$X = c_o - c = 0.822 \pm 0.822 \times 3\% - 0.569 \pm 0.569 \times 5.5\%$$

$$= (0.822 \pm 0.025) - (0.569 \pm 0.031)$$

Therefore, the total uncertainty of X is

$$\pm 0.056/0.235 = \pm 24\%.$$

(c) If the initial concentration (run No. 37) $c_o = 0.776$ mmoles/lit and the final concentration

$$c = 0.182 \text{ mmoles/lit}$$

$$t = 16.6$$

$$T = 960°C$$

Since the contact time is intermediate, an intermediate concentration uncertainty was applied.

$$X = c_o - c = 0.776 \pm 0.776 \times 2\% - 0.182 \pm 0.182 \times 6\%$$

$$= (0.776 \pm 0.016) - (0.182 \pm 0.011) = 0.594 \pm 0.027$$

Therefore, the total uncertainty in X is

$$\pm 0.027/0.594 = \pm 4.5\%$$

The uncertainty in a calculated rate (X/t) value for a low contact time and low extent of reaction is

38 + 0.7 = 39%. For a high contact time and high extent of reaction, the uncertainty in the rate is 24 + 2.7 = 27%. Thus, there is a leveling effect since high flow rates, which correspond to low uncertainties in concentration, produce low extents of reaction, which yield high uncertainties due to small values of X and vice versa. However, as seen from the above example, the uncertainty in X overpowers that of the contact time. Example (c) illustrates the powerful effect that a very high extent of reaction has on the total uncertainty in the rate i.e., 4.5 + 2.7 = 7.2%.

Thus, rate values, calculated from low temperature experiments would have a probable maximum uncertainty of about 40%, where those resulting from high temperature experiments would have a lower maximum uncertainty of less than 10%.

8) The above calculations describe the maximum deviation from the mean that a data point can have under a particular set of conditions and are tabulated below as predicted uncertainty. Rate constants, first and second-order, were calculated from least square intercepts and slopes respectively of plots of r/c versus c where $r = k_1 c + k_2 c^2$. Values are tabulated below:

Temp. °C	Mean values k_1	k_2	Predicted (max.) uncertainty		Observed deviation (95% confid. level)	
880	0.016	0.006	±0.004	±0.001	±0.003	±0.001 (20%)
910	0.033	0.019	±0.008	±0.004	±0.008	±0.004 (23%)
940	0.067	0.126	±0.015	±0.029	±0.007	±0.014 (11%)
960	0.147	0.198	±0.034	±0.046	±0.031	±0.041 (21%)

It can be seen that the observed deviations (95% confidence level) fall within the range predicted from the treatment of uncertainties.

APPENDIX D

Procedure for Determining the Hydrogen Cyanide in the Exit Stream

As stated earlier, it was felt that this pyrolysis reaction could be followed by determining the hydrogen cyanide in the reactor exit stream. For this procedure to be valid, all or some constant fraction of the CN (resulting from decomposition) would have had to appear as HCN in exit stream. Experimental results indicated that this was not the case; therefore, the method was abandoned as a means of following the reaction under study.

This procedure is a modification of the Liebig method[16] for soluble cyanides. The pre-end point reaction was as follows:

$$Ag^{+} + 2CN^{-} \longrightarrow Ag(CN)_2^{-}$$

The first appearance of permanent turbidity signaled the equivalence point. For obvious reasons, this was very difficult to detect. To minimize the inherent uncertainty in such a determination, an instrumental method was devised to perform the titration and detect the reaction's end point. A schematic showing the basic components is shown in Figure 11. The Sargent constant-rate

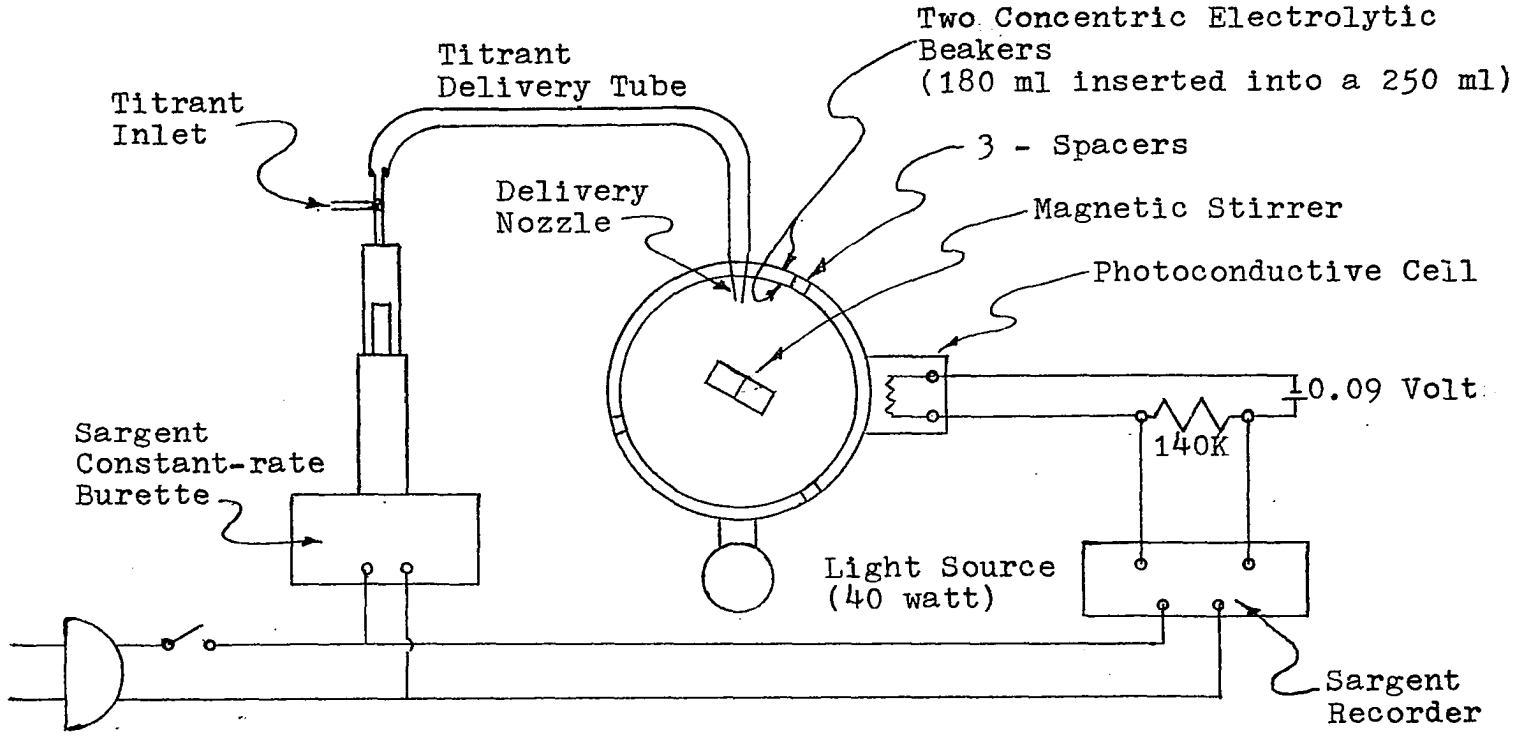

Figure 11 Instrument for Determining Cyanide Ion.

burette added titrant i.e., standardized $AgNO_3$, and at the equivalence point permanent turbidity appeared and was detected by a photoconductive cell located at 90 degrees to a light source. Thus, it was the light scattered by the first appearance of AgCN precipitate which signaled the end point. Changes in the resistance across the photoconductive cell altered the current in the circuit; thus, the potential across the 140K resistor affected recorder displacement. This technique produced results of high reproducibility i.e., maximum uncertainty of 1.0 per cent.

Procedure

Two fritted glass bubble towers were placed in series immediately downstream from the reactor. About 100 ml of 0.05M KOH was placed in each bubbler so as to quantitatively trap hydrogen cyanide from the exit gas stream. It was found experimentally that about 98 per cent of the hydrogen cyanide was trapped in the first bubbler and trapping was virtually complete with the second bubbler. The trapping reaction was as follows:

$$KOH + HCN \longrightarrow H_2O + KCN$$

No appreciable amount of hydrolysis of the trapped unreacted acetonitrile occurred. The contents of the bubblers was rinsed into a 250 ml volmetric flask, and the volume

was made up to 250 ml. Aliquots were pipetted into a beaker for subsequent titration. The silver nitrate titrant was standardized each day with a potassium cyanide standard. The Sargent constant rate burette delivered titrant at a rate of 5.00 ml/min and the time required for attainment of the end point was indicated by the length of chart between the starting point and the point of pen displacement. The burette and the chart drive motor were actuated simultaneously by a simple switch. The number of mmoles of hydrogen cyanide per given aliquot was calculated as follows:

$$\frac{\text{titrant addition rate}}{\text{chart speed} \times \text{length of chart}} \times \text{normality of titrant} = \text{number of mmoles of HCN}$$

BIBLIOGRAPHY

1. B. S. Rabinovitch and C. A. Winkler, Can. J. Res., 20, B, 69-72, 1942.

2. D. E. McElcheran, M. H. J. Wijnen, and E. W. R. Steacie, Can. J. Chem., 36, 321-9, 1958.

3. M. Hunt, J. A. Kerr, and A. F. Trotman-Dickenson, J. Chem. Soc., 5074, 1965.

4. D. Hale, L. Harrah, R. Rondeau, and S. Zakanycz, Develop. Appl. Spectroscopy, 3, 361-71, 1963.

5. T. F. Doumani and C. S. Coe, U.S. 2,983,099 (1961).

6. Leonide Andrussow, Chim. Ind. (Paris), 86, 542-5, 1961.

7. J. M. Sullivan and T. J. Houser, Chem. and Ind., 1057, 1965.

8. "Handbook of Chemistry and Physics", 45th ed., The Chemical Rubber Company, 1964-5, E-49.

9. T. J. Houser, "The Kinetics of the Thermal Decomposition of Pentachloroethane", Unpublished Doctor's dissertation, University of Michigan, Ann Arbor, Michigan, 1957, p. vii + 24.

10. C. F. Cullis and J. G. Yates, J. Chem. Soc., 2833, 1964.

11. "JANAF Thermochemical Tables", Dow Chemical Company, 1965.

12. R. I. Reed and W. Snedden, Trans. Faraday Soc., 55, 876-9, 1959.

13. A. E. Messner, D. M. Rosie, and P. A. Argabright, Anal. Chem., 31, 230, 1959.

14. K. J. Laidler, "Chemical Kinetics", 2nd ed., McGraw-Hill, New York, 1965, p. 387.

15. C. Marsden, "Solvents Guide", Cleaver-Hume Press, Ltd., London, 1969, p. 16.

16. Wilfred Scott and N. Howell Furman, "Standard Methods of Chemical Analysis," D. Van Nostrand Company, Inc., New York, vol. 1, p. 39.